Estimates of Primary Ejecta and Local Material for the Orientale Basin on the Moon. M. G. Xie and M.-H. Zhu, Lunar and Planetary Science Laboratory, Macau University of Science and Technology, Taipa, Macau (xieminggang13@gmail.com).

Introduction: The Orientale basin, formed ~ 3.8 billion years ago [1], is the youngest multi-ring basin on the Moon. Due to the relatively young age, the Orientale basin suffered minor geological modification since its formation [2, 3]. Its well-preserved morphology, therefore, provides a best choice to study the thicknesses of primary ejecta and local material for large-scale impact basins on the Moon. In this work, primary ejecta always refers to the ejecta from the Orientale basin, and local material is the pre-existing material on the lunar surface that was excavated and incorporated by the primary ejecta when they landed. The ejecta deposit represents the mixture of primary ejecta and local material. Here, we propose a model that considers the erosion of partially filled pre-Orientale craters (PFPOCs, see Fig. 1) to re-investigate the thickness distribution of primary ejecta and local material of the Orientale basin. The DEM model with a spatial resolution of 256 pixels/degree from LOLA [4] was used for all measurements of elevations.
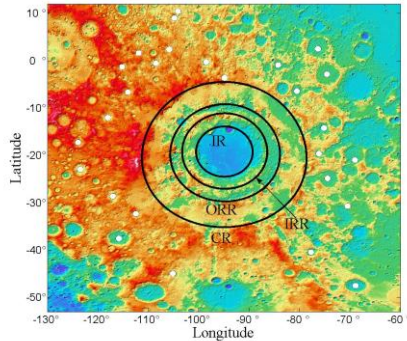

Fig. 1 WAC color shaded relief [5] of Orientale with the locations (white filled circles) where PFPOCs were measured.

Methods: Craters undergo some degree of degradation since its formation because of topographic diffusion arised from the formation of small impact craters [6], and seismic shaking [7-9]. In this work, we assume the topographic diffusion is the main factor accounting for the degradation of complex craters.

In order to accurately estimate the primary ejecta thickness (T_{PE}), and to give a first order estimate of the local material thickness (T_{LM}), we have to consider the erosion of PFPOCs and the crater interior geometry. But the exact crater profile was unknown due to the burial by ejecta deposits, and it means there is another unknown. Fortunately, PFPOCs have two attributes, the exposed rim height (H_{ER}) and average exposed rim-floor depth (D_{AERF}) equaling to the difference of rim elevation to the mean elevation within crater rim, and are both related to the two unknowns. The procedures of our method are illustrated briefly as follows: (1) H_{ER} and D_{AERF} are determined from measurements (see Fig. 2a). (2) we use a variety of initial crater profile to create a variety of degraded profiles that match the crater diameter of each measured PFPOC, and calculate the numerical relations $[T_{PE}, T_{LM}] = F (H_{ER}, D_{AERF})$ for each of these degraded profiles. Local material thickness, T_{LM}, is considered to be the average thickness of infilling material (see the green region within crater rim in Fig. 2b). (3) therefore, measurements and simulations had two parameters in common, and a best fit model was used to match H_{ER} and D_{AERF} of measurements with these of simulations, then T_{PE} and T_{LM} could be determined from the numerical relations. For example, the observed profile (gray dashed line in Fig. 2b) of a typical PFPOC as shown in Fig. 2a has a best-fit profile in Fig. 2b (the blue dotted line).

Results and Disscusions: The model-derived primary ejecta thickness (green filled triangles) and local material thickness (red circles) of each PFPOC are displayed in Fig. 3.

A nonlinear least squares fit to primary ejecta thicknesses using $\delta = T_{PE\_R} (r/R)^{-b}$ (where δ is the thickness at distance r, T_{PE_R} is the primary ejecta thickness at the basin rim, $R = 465$ km is the basin radius, b is the exponent) gives $T_{PE\_R} = 0.85 \pm 0.53$ km and $b = 2.8 \pm 1.9$ (95% confidence intervals) (see the green line). Our result is smaller than previous results [e.g., 10] (the gray dashed line).

Because the material under the impact site is not ejected, the excavation volume is ~ 90% of the paraboloidal excavation cavity [11]. And assuming the porosity of primary ejecta is 20% higher than the target matrial [12], conservation of mass gives:

$$d_{ex} = 3.5556 (R_{TC}/R)^{-b} T_{PE\_R}/(b-2) \qquad (1)$$

where d_{ex} is excavation depth, R_{TC} is transient crater radius at the original ground level. Assuming $d_{ex} = 0.2 R_{TC}$, Eq. (1) gives $d_{ex} = 40$ km, then $R_{TC} = 200$ km for the Orientale basin, consistent with the estimates from gravity inversions [e.g., 13, 14].

The primary ejecta thickness is often defined either by Eq. (2) [15] or (3) [16].

$$\delta = 0.14 R_{TR}^{0.74} (r/R_{TR})^{-3} \qquad (2)$$

$$\delta = 0.033 R_{TR} (r/R_{TR})^{-3} \qquad (3)$$
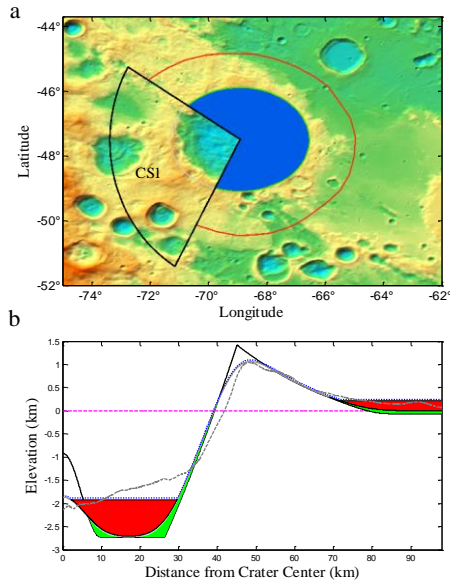
a

b

Fig. 2 An example of fitting results. (a) The red and green lines are used to depict outer surface and rim, respectively. The blue region describes crater interior. CS1 is a circular sector excluded from measurement because of craters formed on and outside of crater rim. (b) The gray curve, which degraded from fresh crater profile (the black curve), is covered by ejecta deposits to form the visible profile (the blue dotted line). Note that red and green regions are both ejecta deposits.
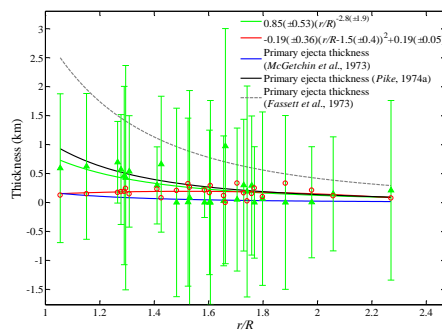

Fig. 3 Distribution of primary ejecta thicknesses (green filled triangles) and local material thicknesses (red circles). The green line represents the best fit of the primary ejecta thicknesses, the red line represents the best fit of the local material thicknesses.

where R_{TR} is rim-to-rim radius of transient crater, and all values are given in meters. Previous works [e.g., 16] considered that transient crater is geometrically similar to fresh simple craters, and the value of R_{TR} is about 1.2 times of R_{TC} [17,16], then R_{TR} is 240 km. For comparison, the thickness distribution of primary ejecta was shown in Fig. 3, in which the blue and black lines were calculated after Eq. (2) and (3), respectively. It turns out that the model-derived primary ejecta thicknesses are consistent with Eq. (3). This result agrees with the measured results of complex craters [18], which implies that Eq. (3) gives a good estimate of primary ejecta thickness for complex craters. Widely

cited Eq. (2) gives a very poor estimate. It might be due to that it was established from inadequate lunar data and inconsistent with the general form of either empirical or theoretical studies of craters [16].

As shown in Fig. 4, the proportion of local material to ejecta deposits increases along the radial distance from the basin center, and ejecta deposits are mostly local material at a distance larger than ~1.5 *R* (this is just a rough estimate due to the scattering of the data points), because primary ejecta thin and excavation efficiency increases outward. This result indicates that the ballistic sedimentation for primary ejecta within ejecta blanket is important for Orientale. And it is even more important for basins larger than Orientale, because the primary ejecta velocity is larger than that of Orientale at the same non-dimensional distance. Therefore, ejecta deposits can not be taken as mostly primary ejecta everywhere [19].
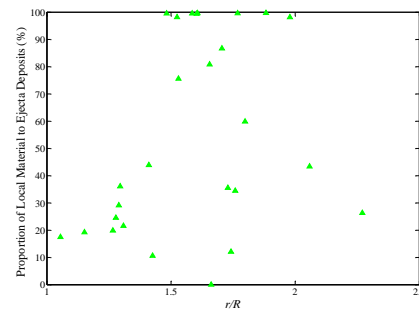

Fig. 4 Proportion of local material to ejecta deposits as a function of non-dimensional distance. Ejecta deposit thickness is the sum of primary ejecta thickness and local material thickness.

References: [1] Greeley et al. (1993), *JGR, 98*(E9), 17,183-17,205. [2] Spudis P. D. (1993), *The Geology of Multi‑Ring Basins*, Cambridge Univ. Press. [3] Kreslavsky M. A. and J. W. Head (2012), *JGR*, 117, E00H24. [4] Smith D. E. et al. (2010), *GRL, 37*, 18. [5] Robinson M. et al. (2010), *SSR*, *150*, 81-124. [6] Soderblom L. A. (1970), *JGR, 75*, 2655-2661. [7] Schultz P., and Gault D. (1975), *LPSC*, *6*, 2845-2862. [8] Richardson J. E. et al. (2004), *Science, 306* , 1526-1529. [9] Richardson J. E. et al. (2005), *Icarus, 179*, 325-349. [10] Fassett C. I. et al. (2011), *GRL*, *38*, L17201. [11] Haskin L. A. et al. (2003), *Meteorit. Planet. Sci., 38*, 13 − 33. [12] Melosh H. J. (1989), *Impact Cratering: A Geologic Process*, Oxford Univ. Press. [13] Wieczorek M. A., and Phillips R. J. (1999), *Icarus, 139*, 246-259. [14] Hikida H., and Wieczorek M. A. (2007), *Icarus, 192*, 150–166. [15] McGetchin T. R. et al. (1973), *EPSL, 20*, 226 − 236. [16] Pike R. J. (1974), *EPSL*, *23*, 265–271. [17] Baldwin R. B. (1963), *The Measure of the Moon*, The University of Chicago Press. [18] Kr ügel T. et al. (2014), *LPSC, Abstract* #1834. [19] Oberbeck V. R. (1975), *Rev. Geophys., 13*, 337–362.